Published for SISSA by Springer

Received: December 6, 2012
Accepted: January 18, 2013
Published: February 7, 2013

Measurement of J/ψ production in pp collisions at $\sqrt{s} = 2.76\,\text{TeV}$

The LHCb collaboration

E-mail: monica.pepe.altarelli@cern.ch

Abstract: The production of J/ψ mesons is studied with the LHCb detector using data from pp collisions at $\sqrt{s} = 2.76\,\text{TeV}$ corresponding to an integrated luminosity of $71\,\text{nb}^{-1}$. The differential cross-section for inclusive J/ψ production is measured as a function of its transverse momentum p_{T}. The cross-section in the fiducial region $0 < p_{\text{T}} < 12\,\text{GeV}/c$ and rapidity $2.0 < y < 4.5$ is measured to be $5.6 \pm 0.1\,(\text{stat}) \pm 0.4\,(\text{syst})\,\mu\text{b}$, with the assumption of unpolarised J/ψ production. The fraction of J/ψ production from b-hadron decays is measured to be $(7.1 \pm 0.6\,(\text{stat}) \pm 0.7\,(\text{syst}))\%$.

Keywords: Quarkonium, Hadron-Hadron Scattering, Flavor physics

ArXiv ePrint: 1212.1045

doi:10.1007/JHEP02(2013)041

JHEP02(2013)041

Contents

JHEP02(2013)041

1 Introduction

This article presents the measurements of the differential inclusive J/ψ production cross-section as a function of the J/ψ transverse momentum, and of the fraction of J/ψ mesons coming from the decay of a b-hadron in pp collisions at a centre-of-mass energy of 2.76 TeV. The study is based on a sample corresponding to an integrated luminosity of $71\,\text{nb}^{-1}$ collected in March 2011 with an average of one visible pp interaction per recorded event. The main goal of this short run was to provide a reference for the study of Pb-Pb interactions carried out at the same centre-of-mass energy per nucleon-nucleon collision.

Studies of J/ψ production have been performed by the LHC experiments using data taken at $\sqrt{s} = 7\,\text{TeV}$ [1–4] as well as at lower energies [5]. The data at $\sqrt{s} = 2.76\,\text{TeV}$ provide an extra measurement to test theoretical models of J/ψ production in hadron collisions and are also used to obtain a measurement of J/ψ production from b-hadron decays.

The LHCb detector [6] is a single-arm forward spectrometer covering the pseudorapidity range $2 < \eta < 5$, designed for the study of particles containing b or c quarks. The detector includes a high precision tracking system consisting of a silicon-strip vertex detector (VELO) surrounding the pp interaction region, a large-area silicon-strip detector located upstream of a dipole magnet with a bending power of about 4 Tm, and three stations of silicon-strip detectors and straw drift tubes placed downstream. Charged hadrons are identified using two ring-imaging Cherenkov detectors. Photon, electron and hadron candidates are identified by a calorimeter system consisting of scintillating-pad and preshower detectors, an electromagnetic calorimeter and a hadronic calorimeter. Muons are identified by a system which consists of five stations of alternating layers of iron and multiwire

proportional chambers, with the exception of the centre of the first station, which uses triple-GEM detectors.

For the data used in this analysis, the VELO, which consists of two retractable halves surrounding the interaction region, was positioned during collisions with its sensitive area at a minimum distance of 13 mm from the beam instead of the nominal 8 mm. This was necessary to provide a larger aperture for the beam at the lower centre-of-mass energy of 2.76 TeV.

The trigger [7] consists of a hardware stage, based on information from the calorimeter and muon systems, followed by a software stage, which applies a full event reconstruction. Only the triggers used in this analysis are described here. At the hardware trigger level, a single muon candidate with p_{T} larger than 0.8 GeV/c is required. In the first stage of the software trigger a simplified event reconstruction is applied and one requires a $\mu^+\mu^-$ candidate with invariant mass greater than 2.7 GeV/c^2. In the second stage a full event reconstruction is performed and only events with a $\mu^+\mu^-$ pair with invariant mass within 120 MeV/c^2 of the known J/ψ mass [8] are retained.

2 Event selection

The analysis strategy is based upon that described in ref. [1]. Candidate J/ψ mesons are formed from pairs of opposite-sign charged particles reconstructed in the fiducial region $2 < \eta < 5$ by the full tracking system using algorithms adapted to the VELO at its displaced position. Each particle must have p_{T} above 0.7 GeV/c and be identified as a muon. The two muons are required to originate from a common vertex, and only candidates with a χ^2 probability of the vertex fit larger than 0.5% are kept. Events are selected in which at least one primary vertex is reconstructed from at least three VELO tracks, excluding the two signal muon tracks from the J/ψ decay. A VELO track is required to have at least three hits on a straight line in the radial strips of the detector.

The Monte Carlo samples used for this analysis are based on the Pythia 6.4 generator [9] configured with the parameters detailed in ref. [10]. The EvtGen package [11] is used to generate hadron decays, in particular for J/ψ and b-hadrons. The interaction of the generated particles with the detector and its response are implemented using the Geant4 toolkit [12, 13] as described in ref. [14]. Radiative corrections to the decay $J/\psi \to \mu^+\mu^-$ are generated using the Photos package [15]. The simulated position of the VELO corresponds to that in the data.

3 Cross-section determination

The differential cross-section for J/ψ production in a p_{T} bin is given by

$$\frac{\mathrm{d}\sigma}{\mathrm{d}p_{\mathrm{T}}} = \frac{N\left(J/\psi \to \mu^+\mu^-\right)}{\mathcal{L} \times \epsilon_{\mathrm{tot}} \times \mathcal{B}\left(J/\psi \to \mu^+\mu^-\right) \times \Delta p_{\mathrm{T}}}\,, \tag{3.1}$$

where $N\left(J/\psi \to \mu^+\mu^-\right)$ is the number of observed $J/\psi \to \mu^+\mu^-$ signal decays in the given bin, ϵ_{tot} the J/ψ detection efficiency per p_{T} bin (including both acceptance and trigger),

JHEP02(2013)041

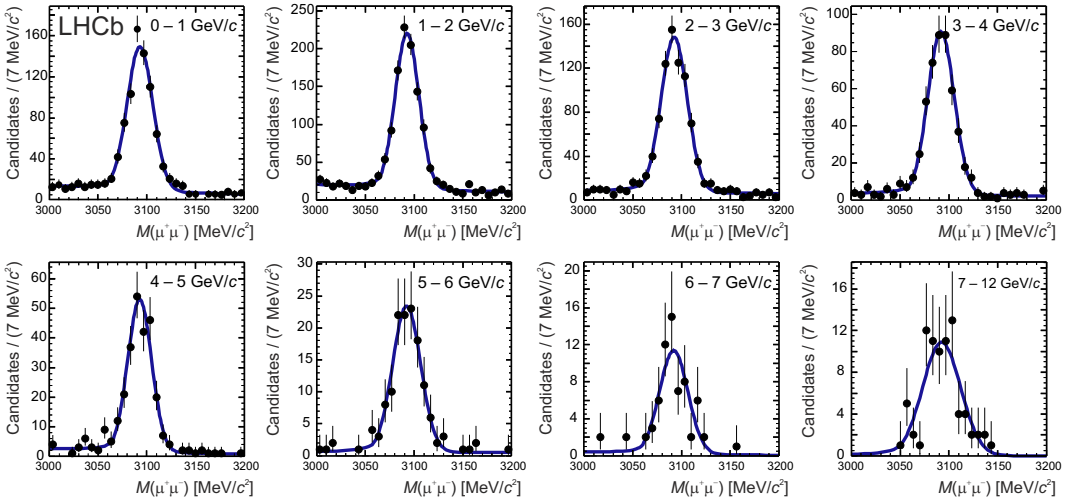

Figure 1. Dimuon mass distributions, with fit results superimposed, in bins of p_{T}. Results for $p_{\mathrm{T}} > 7\,\mathrm{GeV}/c$ are merged in the last bin.

$\mathcal{L}$ the integrated luminosity, $\mathcal{B}(J/\psi \to \mu^+\mu^-) = (5.93 \pm 0.06) \times 10^{-2}$ [8] the branching fraction of the $J/\psi \to \mu^+\mu^-$ decay, and Δp_{T} the p_{T} bin size.

The number of signal J/ψ mesons per p_{T} bin is determined from an extended unbinned maximum likelihood fit to the invariant mass distribution of the reconstructed J/ψ candidates in the interval $3.0 < M_{\mu\mu} < 3.2\,\mathrm{GeV}/c^2$, where the signal is described by a Crystal Ball function [16] and the combinatorial background by an exponential distribution. Figure 1 shows the J/ψ invariant mass distribution together with the fit results for each p_{T} bin, where results for $7 < p_{\mathrm{T}} < 12\,\mathrm{GeV}/c$ are merged in the last bin.

There are two main sources that contribute to the inclusive J/ψ sample. Those produced at the pp collision point, either directly or from the decay of a directly produced higher mass charmonium state, are called prompt J/ψ. The second source, J/ψ from b, are those produced in the decay of a b-hadron. Their production is displaced from the pp collision point because of the relatively large b lifetime. The two sources are statistically separated using the measured J/ψ pseudo-decaytime, defined as

$$t_z = \frac{(z_{J/\psi} - z_{\mathrm{PV}}) \times M_{J/\psi}}{p_z}\,, \tag{3.2}$$

where $z_{J/\psi}$ and z_{PV} are the positions along the beam axis of the J/ψ decay vertex and of the primary vertex refitted after removing the two muon tracks from the J/ψ candidate; p_z is the measured J/ψ momentum in the beam direction and $M_{J/\psi}$ the known J/ψ mass [8]. Given that b-hadrons are not fully reconstructed, the J/ψ momentum is used instead of the exact b-hadron momentum and the t_z variable provides a good estimate of the b-hadron decaytime.

The fraction of J/ψ from b is determined from a simultaneous fit to the total pseudo-decaytime t_z and $\mu^+\mu^-$ invariant mass. Due to the small number of J/ψ candidates, the fraction of J/ψ from b is computed over the full p_{T} interval from 0 to 12 GeV/c. The signal decaytime distribution is described by a delta function at $t_z = 0$ for the prompt J/ψ

JHEP02(2013)041

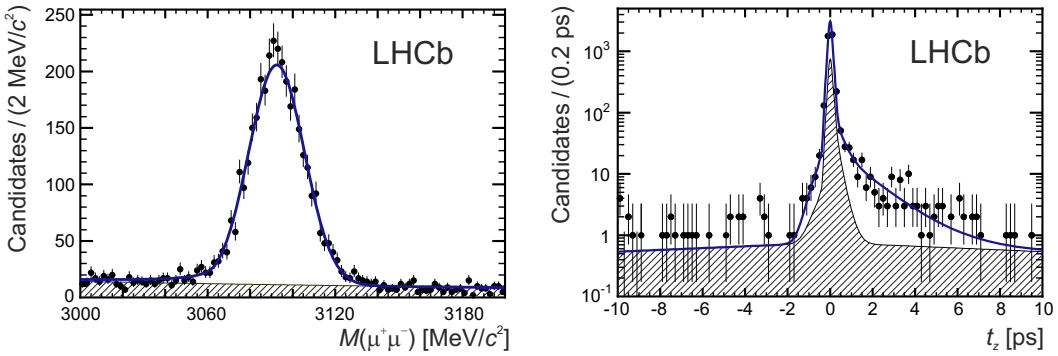

Figure 2. Distributions of the data with projections of the fit superimposed for (left) the dimuon invariant mass and (right) t_z. The thick blue line is the total fit function and the hatched area the background component.

component and an exponential decay function for the J/ψ from b component. The function describing the t_z distribution of the signal is therefore

$$f_{\rm signal}(t_z; f_{\rm p}, f_{\rm b}, \tau_{\rm b}) = f_{\rm p}\,\delta(t_z) + \theta(t_z) f_{\rm b} \frac{e^{-\frac{t_z}{\tau_{\rm b}}}}{\tau_{\rm b}}\,, \tag{3.3}$$

where $\theta(t_z)$ is the step function, $f_{\rm p}$ and $f_{\rm b}$ are the fractions of prompt J/ψ and J/ψ from b in the sample, and $\tau_{\rm b}$ the b-hadron pseudo-lifetime. In the fit, τ_b is fixed to the value of 1.52 ps, as obtained from simulation. The prompt and b components of the signal function are convolved with a triple-Gaussian resolution function

$$f_{\rm res}(t_z; \mu, \sigma_1, \sigma_2, \sigma_3, \beta, \beta') = \frac{\beta}{\sqrt{2\pi}\sigma_1} e^{-\frac{(t_z-\mu)^2}{2\sigma_1^2}} + \frac{\beta'}{\sqrt{2\pi}\sigma_2} e^{-\frac{(t_z-\mu)^2}{2\sigma_2^2}} + \frac{1-\beta-\beta'}{\sqrt{2\pi}\sigma_3} e^{-\frac{(t_z-\mu)^2}{2\sigma_3^2}}\,. \tag{3.4}$$

The parameter μ is the bias of the t_z measurement, and β and β' the fractions of the first two Gaussian functions. The background consists of random combinations of muons from semi-leptonic b and c decays, which tend to produce positive t_z values, as well as of mis-reconstructed tracks from decays in flight of kaons and pions, which contribute both to positive and negative t_z values. The background t_z distribution is parameterised with an empirical function based on the shape obtained from the J/ψ mass sidebands. It is taken as the sum of a delta function and three exponential components, two for positive t_z and one for negative t_z. The exponential parameter, $\tau_{\rm L}$, is common to the larger positive and negative lifetime exponential components. The explicit form is

$$f_{\rm bckg}(t_z) = (1 - f_1 - f_{\rm L})\,\delta(t_z) + \theta(t_z) f_1 \frac{e^{-\frac{t_z}{\tau_1}}}{\tau_1} + f_{\rm L} \frac{e^{-\frac{|t_z|}{\tau_{\rm L}}}}{2\tau_{\rm L}}, \tag{3.5}$$

and is convolved with the same resolution function $f_{\rm res}$ as the signal.

The function used to describe the t_z distribution is therefore

$$f(t_z; f_{\rm p}, f_{\rm b}, \mu, \sigma_1, \sigma_2, \sigma_3, \beta, \beta', \tau_{\rm b}) = \left(f_{\rm p}\,\delta(t_z) + f_{\rm b}\,\frac{e^{-\frac{t_z}{\tau_{\rm b}}}}{\tau_{\rm b}} + (1 - f_{\rm p} - f_{\rm b})\, f_{\rm bckg}(t_z) \right) \otimes f_{\rm res}(t_z; \mu, \sigma_1, \sigma_2, \sigma_3, \beta, \beta')\,, \tag{3.6}$$

JHEP02(2013)041

where all parameters except $\tau_{\rm b}$ are freely varied. The total fit function is the sum of the products of the mass and t_z fit functions for the signal and background. Figure 2 shows the distributions of the dimuon invariant mass and t_z with the projections of the fit superimposed. The invariant mass resolution is $13.0 \pm 0.3\,\mathrm{MeV}/c^2$. The parameter μ describing the bias of the t_z resolution function is 2.3 ± 2.0 fs and the RMS of the t_z resolution function is 84 fs. As a measure of the fit quality, a χ^2 is calculated using a binned event distribution. The resulting fit probability for the t_z distribution is 90%. The fit gives a total yield of 3399 ± 65 J/ψ signal decays.

The fraction of signal J/ψ coming from b-hadron decays is measured to be $F_{\rm b} = \frac{f_b}{f_p+f_b} = (6.7 \pm 0.6)\%$. An absolute correction of 0.4% is applied based on simulation to take into account a bias produced by events in which b-hadron decay products, other than the muons from the J/ψ, are wrongly used to reconstruct the primary vertex. This leads to the result $F_{\rm b} = (7.1 \pm 0.6)\%$ where the uncertainty is only statistical.

A simulated sample of inclusive, unpolarised J/ψ mesons is used to estimate the geometrical acceptance in each $p_{\rm T}$ bin. The reconstruction efficiency, which combines the J/ψ meson detection, reconstruction and selection efficiencies, is also computed from simulation as a function of $p_{\rm T}$ and is corrected to account for the difference observed in the tracking efficiency between data and simulation at $\sqrt{s} = 7\,\mathrm{TeV}$. This correction is about 1%. The efficiency of the hardware trigger is determined directly from data using a large inclusive J/ψ sample at $\sqrt{s} = 7\,\mathrm{TeV}$ triggered and selected with the same requirements as those used in this analysis: the efficiency is calculated in small bins of the J/ψ transverse momentum and rapidity and weighted according to the $p_{\rm T}$ and y distributions as given by the simulation at 2.76 TeV. The efficiency of the software trigger, which makes use of the VELO information, is determined from simulation since the data at $\sqrt{s} = 7\,\mathrm{TeV}$ were taken with the VELO in the closed position. The total efficiency, calculated as the product of acceptance, reconstruction and trigger efficiencies, and its components are displayed in figure 3 as a function of $p_{\rm T}$. A non-zero polarisation of the J/ψ at production can affect the total efficiency [1]. The results quoted in this article assume that the J/ψ mesons are produced unpolarised.

4 Luminosity determination

To determine the integrated luminosity, an effective interaction rate is continuously measured during data taking and an absolute calibration is performed with a dedicated van der Meer (VDM) scan [17]. The strategy is similar to that developed for the $\sqrt{s} = 7\,\mathrm{TeV}$ running [18].

The VDM method exploits the ability to move the beams in both transverse coordinates with high precision and thus to scan the colliding beams with respect to each other. The limiting systematic uncertainty affecting the VDM measurement arises from the knowledge of the number of protons in the colliding bunch pairs. These are measured with two types of beam current transformers installed in the LHC [19–21]. The DCCT (DC Current Transformer) measures the total beam current, and is thus used to constrain the total number of particles. The uncertainty associated with the DCCT calibration is 2.7% [22–

JHEP02(2013)041

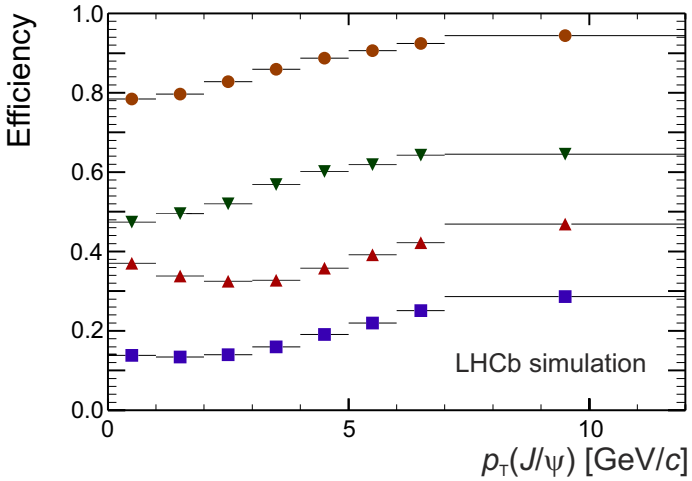

Figure 3. Acceptance (orange circles), reconstruction (upward-facing red triangles), trigger (downward-facing green triangles) and total (blue squares) J/ψ efficiency, as a function of p_T. The efficiencies are evaluated from a Monte Carlo simulation in which the J/ψ is produced unpolarised.

Uncertainty on relative normalisation	
Counter stability	0.5
μ variation among bunch crossings	0.5
Uncertainty on absolute normalisation	
Statistical error of the VDM scan	0.2
Total beam current	2.7
Individual bunch population	0.9
Protons outside nominal bunches	0.4
Length scale calibration	1.0
Non-reproducibility in similar scans at $\sqrt{s} = 7\,\text{TeV}$	2.1
Total uncertainty	3.8

Table 1. Relative systematic uncertainties on the luminosity (%).

24]. The other transformer, the FBCT (Fast Beam Current Transformer) is used to measure the relative charges of the individual bunches. The uncertainty in its offset and linearity contributes a 0.9% uncertainty to the overall luminosity [22–24]. A small fraction of protons in the LHC may be captured outside the nominally filled bunch slots. This contribution, which needs to be subtracted from the DCCT measurement, is estimated to be 2.5% from the number of beam-gas events in nominally empty bunch crossings. Due to the small number of such events and uncertainties in the trigger efficiency, the subtraction introduces a cross-section uncertainty of 0.4%. The uncertainty in the length-scale calibration, which affects the beam separation values, contributes 1% to the systematic uncertainty in the luminosity. Finally, a 2.1% uncertainty is assigned to account for a non-reproducibility of

JHEP02(2013)041

the VDM results observed when performing similar luminosity calibration measurements at $\sqrt{s} = 7\,\text{TeV}$, as decribed in ref. [18].

The integrated luminosity for the runs considered in this analysis is measured to be $70.6 \pm 2.7\,\text{nb}^{-1}$. A summary of the contributions to the overall luminosity uncertainty is provided in table 1. The uncertainties are uncorrelated and therefore added in quadrature.

5 Systematic uncertainties

The different contributions to the systematic uncertainty affecting the cross-section measurement are summarised in table 2. Correction factors estimated directly from data to take into account residual differences between simulation and data are also detailed.

The influence of the choice of the fit function used to describe the shape of the dimuon mass distribution is estimated by fitting the J/ψ invariant mass distribution with the sum of two Crystal Ball functions. The relative difference of 2.2% in the number of signal events is taken as systematic uncertainty.

A fraction of J/ψ events have a lower mass because of the radiative tail. Based on Monte Carlo studies, 5% of the J/ψ signal is estimated to be outside the analysis mass window ($M_{\mu\mu} < 3.0\,\text{GeV}/c^2$) and not counted as signal. The fitted signal yields are therefore corrected, and an uncertainty of 1% is assigned to the cross-section measurement based on a comparison between the radiative tail observed in data and simulation.

To cross-check and assign a systematic uncertainty to the Monte Carlo determination of the muon identification efficiency, the single track muon identification efficiency is measured on data using a tag-and-probe method. This method reconstructs J/ψ candidates in which one muon is identified by the muon system ("tag") and the other one ("probe") is identified by selecting a track with a minimum-ionising energy deposition in the calorimeters. The absolute muon identification efficiency is then evaluated on the probe muon, as a function of the muon momentum and found to be larger than 95%. The ratio of the muon identification efficiency measured in data to that obtained in the simulation is convolved with the momentum distribution of muons from J/ψ to obtain an efficiency correction. This factor is found to be 1.024 ± 0.011 and is consistent with being constant over the full J/ψ transverse momentum and rapidity range; the error on the correction factor is included as a systematic uncertainty.

Studies at $\sqrt{s} = 7\,\text{TeV}$ have shown that the Monte Carlo simulation reproduces the determination from data of the efficiency to reconstruct the two muon tracks from the J/ψ decay within 0.8% to 1.1%, depending on the J/ψ transverse momentum. This difference is taken as a systematic uncertainty. An additional uncertainty of 1% per track is assigned to cover differences in the efficiency of the track χ^2/ndf cut between data and simulation. Similarly, for the selection based on the J/ψ vertex χ^2 probability, a difference below 0.3% is measured between the cut efficiency computed in data and simulation, which is assigned as systematic uncertainty. To take into account the model dependence of the simulation in the efficiency calculation, the main parameters of the Pythia 6.4 generator related to prompt J/ψ production were varied. These parameters define the minimum p_{T} cut-offs for regularising the cross-section. A 4.5% effect on the total efficiency was observed.

JHEP02(2013)041

Source	Systematic uncertainty
Correlated between bins	
Mass fits	2.2
Radiative tail	1.0
Muon identification	1.1
Tracking efficiency	0.8 to 1.1
Track χ^2	2.0
Vertexing	0.3
Model dependence	4.5
$\mathcal{B}(J/\psi \to \mu^+\mu^-)$	1.0
Luminosity	3.8
Uncorrelated between bins	
Trigger	1.6 to 7.7
Applied only to J/ψ from b fraction	
t_z fit	10.0
Applied only to $\sigma(pp \to b\bar{b}X)$	
$\mathcal{B}(b \to J/\psi\, X)$	8.6

Table 2. Relative systematic uncertainties on the cross-section results and on the fraction of J/ψ mesons from b-hadron decay (%).

The hardware trigger efficiency is determined using a sample of events at $\sqrt{s} = 7\,\text{TeV}$ that would still be triggered if the J/ψ candidate were removed. The software trigger efficiency is obtained from the simulation. Its uncertainty is evaluated by comparing true and measured trigger efficiency using a trigger-unbiased sample of simulated J/ψ events.

Uncertainties related to the t_z fit procedure are taken into account by varying the slope of the exponential function of the J/ψ from b component by its uncertainty in the simulation (2%). The resulting 10% variation of the number of J/ψ from b is used as a systematic uncertainty that affects the measurement of F_b. The influence of the background parametrisation was studied by varying the number of exponential functions in eq. (3.5) and found to be negligible. Furthermore, an uncertainty of 8.6% on the average branching fraction of b decays to a final state containing a J/ψ meson contributes to the uncertainty on the extrapolation to the total $b\bar{b}$ cross-section.

6 Results

The measured differential cross-section for inclusive J/ψ production as a function of p_T, after all corrections and assuming no polarisation, is given in table 3 and displayed in figure 4. The integrated inclusive cross-section for J/ψ production in the defined fiducial

JHEP02(2013)041

$p_{\rm T}$ (GeV/c)	dσ/d$p_{\rm T}$ [nb/(GeV/c)]
0−1	$1270 \pm 60 \pm 130$
1−2	$1780 \pm 70 \pm 160$
2−3	$1290 \pm 50 \pm 90$
3−4	$700 \pm 40 \pm 50$
4−5	$313 \pm 22 \pm 24$
5−6	$142 \pm 13 \pm 10$
6−7	$61 \pm 8 \pm 4$
7−12	$14 \pm 2 \pm 1$

Table 3. Differential cross-section dσ/d$p_{\rm T}$ at $\sqrt{s} = 2.76$ TeV for inclusive J/ψ production in bins of $p_{\rm T}$. The rapidity range covered is $2.0 < y < 4.5$. The first uncertainty is statistical and the second is systematic.

region is

$$\sigma\,(J/\psi,\, p_{\rm T} < 12\ {\rm GeV}/c,\, 2.0 < y < 4.5) \;=\; 5.6 \pm 0.1 \pm 0.4\,\mu{\rm b}.$$

The first uncertainty is statistical and the second systematic. Studies indicate that this result could change by up to 20% assuming fully longitudinal or fully transverse J/ψ polarisation [1]. The fraction of J/ψ from b is measured to be

$$F_b = (7.1 \pm 0.6 \pm 0.7)\%$$

in the same acceptance range, $p_{\rm T} < 12\,{\rm GeV}/c$ and $2.0 < y < 4.5$.

From the above results, one can deduce

$$\sigma\,(J/\psi \text{ from } b,\, p_{\rm T} < 12\ {\rm GeV}/c,\, 2.0 < y < 4.5) \;=\; 400 \pm 35 \pm 49\,{\rm nb},$$

in good agreement with the theoretical prediction of 370^{+170}_{-110} nb, based on NLO calculations described in ref. [25]. In addition, the total $b\bar{b}$ production cross-section is computed as

$$\sigma(pp \to b\bar{b}X) = \alpha_{4\pi}\,\frac{\sigma\,(J/\psi,\, p_{\rm T} < 12\ {\rm GeV}/c,\, 2.0 < y < 4.5) \times F_{\rm b}}{2\,\mathcal{B}(b \to J/\psi\, X)}, \qquad (6.1)$$

where the factor $\alpha_{4\pi} = 6.3$ is an extrapolation factor of the cross-section from the measured to the full kinematic region. This factor is obtained using the simulation software described previously. The inclusive $b \to J/\psi\, X$ branching fraction is $\mathcal{B}(b \to J/\psi\, X) = (1.16 \pm 0.10)\%$ [8]. The resulting total $b\bar{b}$ cross-section is $\sigma(pp \to b\bar{b}X) = 110 \pm 9 \pm 16\,\mu$b. No systematic uncertainty has been included for the extrapolation factor $\alpha_{4\pi}$ estimated from the simulation. The value of the extrapolation factor given by NLO calculations is 6.1 [25].

7 Conclusions

The differential cross-section for inclusive J/ψ production is measured as a function of the J/ψ transverse momentum in the forward region, $2.0 < y < 4.5$. The analysis is based on

JHEP02(2013)041

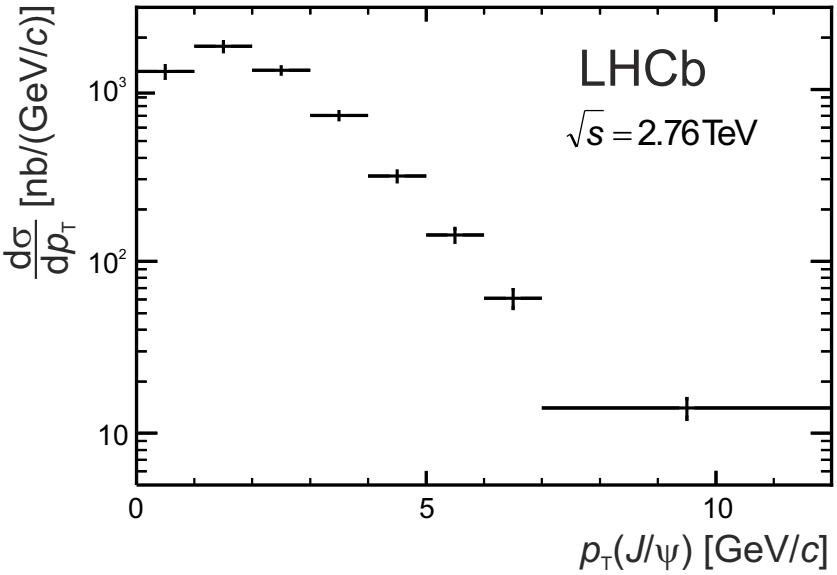

Figure 4. Differential production cross-section for inclusive J/ψ production in the rapidity range $2.0 < y < 4.5$ as a function of $p_{\rm T}$. The vertical error bars are the quadratic sums of the statistical and systematic uncertainties.

a data sample corresponding to an integrated luminosity of $71\,\text{nb}^{-1}$ collected by the LHCb experiment at the Large Hadron Collider at a centre-of-mass energy of $\sqrt{s} = 2.76\,\text{TeV}$. The results obtained are in good agreement with earlier measurements of the inclusive J/ψ production cross-section in pp collisions at the same centre-of-mass energy, performed by ALICE in the region $2.5 < y < 4.0$ [26]. A first measurement of the production of J/ψ from b-hadron decays at 2.76 TeV is also obtained.

Acknowledgments

We thank M. Cacciari for providing theoretical predictions of the $b\bar{b}$ production cross-section in the LHCb acceptance. We express our gratitude to our colleagues in the CERN accelerator departments for the excellent performance of the LHC. We thank the technical and administrative staff at the LHCb institutes. We acknowledge support from CERN and from the national agencies: CAPES, CNPq, FAPERJ and FINEP (Brazil); NSFC (China); CNRS/IN2P3 and Region Auvergne (France); BMBF, DFG, HGF and MPG (Germany); SFI (Ireland); INFN (Italy); FOM and NWO (The Netherlands); SCSR (Poland); ANCS/IFA (Romania); MinES, Rosatom, RFBR and NRC "Kurchatov Institute" (Russia); MinECo, XuntaGal and GENCAT (Spain); SNSF and SER (Switzerland); NAS Ukraine (Ukraine); STFC (United Kingdom); NSF (USA). We also acknowledge the support received from the ERC under FP7. The Tier1 computing centres are supported by IN2P3 (France), KIT and BMBF (Germany), INFN (Italy), NWO and SURF (The Netherlands), PIC (Spain), GridPP (United Kingdom). We are thankful for the computing resources put at our disposal by Yandex LLC (Russia), as well as to the communities behind the multiple open source software packages that we depend on.

JHEP02(2013)041

References

[1] LHCb collaboration, *Measurement of J/ψ production in pp collisions at $\sqrt{s} = 7$ TeV*, *Eur. Phys. J.* **C 71** (2011) 1645 [arXiv:1103.0423] [INSPIRE].

[2] ALICE collaboration,*Rapidity and transverse momentum dependence of inclusive J/ψ production in pp collisions at $\sqrt{s} = 7$ TeV*, *Phys. Lett.* **B 704** (2011) 442 [*Erratum ibid.* **B 718** (2012) 692-698] [arXiv:1105.0380] [INSPIRE].

[3] ATLAS collaboration, *Measurement of the differential cross-sections of inclusive, prompt and non-prompt J/ψ production in proton-proton collisions at $\sqrt{s} = 7$ TeV*, *Nucl. Phys.* **B 850** (2011) 387 [arXiv:1104.3038] [INSPIRE].

[4] CMS collaboration, *J/ψ and ψ_{2S} production in pp collisions at $\sqrt{s} = 7$ TeV*, *JHEP* **02** (2012) 011 [arXiv:1111.1557] [INSPIRE].

[5] N. Brambilla et al., *Heavy quarkonium: progress, puzzles and opportunities*, *Eur. Phys. J.* **C 71** (2011) 1534 [arXiv:1010.5827] [INSPIRE].

[6] LHCb collaboration, *The LHCb detector at the LHC*, 2008 *JINST* **3** S08005 [INSPIRE].

[7] R. Aaij et al., *The LHCb trigger and its performance*, arXiv:1211.3055 [INSPIRE].

[8] Particle Data Group collaboration, J. Beringer et al., *Review of particle physics*, *Phys. Rev.* **D 86** (2012) 010001 [INSPIRE].

[9] T. Sjöstrand, S. Mrenna and P.Z. Skands, *PYTHIA 6.4 physics and manual*, *JHEP* **05** (2006) 026 [hep-ph/0603175] [INSPIRE].

[10] I. Belyaev et al., *Handling of the generation of primary events in* Gauss*, the LHCb simulation framework*, *IEEE Nucl. Sci. Symp. Conf. Rec.* (2010) 1155.

[11] D. Lange, *The EvtGen particle decay simulation package*, *Nucl. Instrum. Meth.* **A 462** (2001) 152 [INSPIRE].

[12] GEANT4 collaboration, J. Allison et al., *GEANT4 developments and applications*, *IEEE Trans. Nucl. Sci.* **53** (2006) 270.

[13] GEANT4 collaboration, S. Agostinelli et al., *GEANT4: a simulation toolkit*, *Nucl. Instrum. Meth.* **A 506** (2003) 250 [INSPIRE].

[14] M. Clemencic et al., *The LHCb simulation application,* Gauss*: design, evolution and experience*, *J. Phys. Conf. Ser.* **331** (2011) 032023.

[15] P. Golonka and Z. Was, *PHOTOS Monte Carlo: A Precision tool for QED corrections in Z and W decays*, *Eur. Phys. J.* **C 45** (2006) 97 [hep-ph/0506026] [INSPIRE].

[16] T. Skwarnicki, *A study of the radiative cascade transitions between the Υ' and Υ resonances*, Ph.D. thesis, Institute of Nuclear Physics, Krakow, Poland (1986) [DESY-F31-86-02]

[17] S. van der Meer, *Calibration of the effective beam height in the ISR*, ISR-PO-68-31 (1968).

[18] LHCb collaboration, *Absolute luminosity measurements with the LHCb detector at the LHC*, 2012 *JINST* **7** P01010 [arXiv:1110.2866] [INSPIRE].

JHEP02(2013)041

[19] J. Gras, M. Ludwig and P. Odier, *The 2010 LHC DC BCT measurement system and its main sources of uncertainties*, CERN-LHC-Project-Note-432 (2010).

[20] D. Belohrad, J. Gras and M. Ludwig, *The 2010 LHC ring Fast BCT measurement system and its main sources of uncertainties*, CERN-LHC-Project-Note-433 (2010).

[21] D. Belohrad et al., *Commissioning and first performance of the LHC beam current measurement systems*, in the proceedings of the 1st *International Particle Accelerator Conference (IPAC10)*, May 23–28, Kyoto, Japan (2010).

[22] G. Anders et al., *LHC bunch current normalisation for the April-May 2010 luminosity calibration measurements*, CERN-ATS-Note-2011-004 (2011).

[23] G. Anders et al., *LHC bunch current normalisation for the October 2010 luminosity calibration measurements*, CERN-ATS-Note-2011-016 (2011).

[24] C. Ohm and T. Pauly, *The ATLAS beam pick-up based timing system*, *Nucl. Instrum. Meth.* **A 623** (2010) 558 [arXiv:0905.3648] [INSPIRE].

[25] M. Cacciari et al., *Theoretical predictions for charm and bottom production at the LHC*, *JHEP* **10** (2012) 137 [arXiv:1205.6344] [INSPIRE].

[26] ALICE collaboration, *Inclusive J/ψ production in pp collisions at $\sqrt{s} = 2.76$ TeV*, *Phys. Lett.* **B 718** (2012) 295 [arXiv:1203.3641] [INSPIRE].

JHEP02(2013)041

The LHCb collaboration

R. Aaij[38], C. Abellan Beteta[33,n], A. Adametz[11], B. Adeva[34], M. Adinolfi[43], C. Adrover[6], A. Affolder[49], Z. Ajaltouni[5], J. Albrecht[35], F. Alessio[35], M. Alexander[48], S. Ali[38], G. Alkhazov[27], P. Alvarez Cartelle[34], A.A. Alves Jr[22,35], S. Amato[2], Y. Amhis[7], L. Anderlini[17,f], J. Anderson[37], R. Andreassen[57], R.B. Appleby[51], O. Aquines Gutierrez[10], F. Archilli[18], A. Artamonov [32], M. Artuso[53], E. Aslanides[6], G. Auriemma[22,m], S. Bachmann[11], J.J. Back[45], C. Baesso[54], V. Balagura[28], W. Baldini[16], R.J. Barlow[51], C. Barschel[35], S. Barsuk[7], W. Barter[44], A. Bates[48], Th. Bauer[38], A. Bay[36], J. Beddow[48], I. Bediaga[1], S. Belogurov[28], K. Belous[32], I. Belyaev[28], E. Ben-Haim[8], M. Benayoun[8], G. Bencivenni[18], S. Benson[47], J. Benton[43], A. Berezhnoy[29], R. Bernet[37], M.-O. Bettler[44], M. van Beuzekom[38], A. Bien[11], S. Bifani[12], T. Bird[51], A. Bizzeti[17,h], P.M. Bjørnstad[51], T. Blake[35], F. Blanc[36], C. Blanks[50], J. Blouw[11], S. Blusk[53], A. Bobrov[31], V. Bocci[22], A. Bondar[31], N. Bondar[27], W. Bonivento[15], S. Borghi[51], A. Borgia[53], T.J.V. Bowcock[49], E. Bowen[37], C. Bozzi[16], T. Brambach[9], J. van den Brand[39], J. Bressieux[36], D. Brett[51], M. Britsch[10], T. Britton[53], N.H. Brook[43], H. Brown[49], A. Büchler-Germann[37], I. Burducea[26], A. Bursche[37], J. Buytaert[35], S. Cadeddu[15], O. Callot[7], M. Calvi[20,j], M. Calvo Gomez[33,n], A. Camboni[33], P. Campana[18,35], A. Carbone[14,c], G. Carboni[21,k], R. Cardinale[19,i], A. Cardini[15], H. Carranza-Mejia[47], L. Carson[50], K. Carvalho Akiba[2], G. Casse[49], M. Cattaneo[35], Ch. Cauet[9], M. Charles[52], Ph. Charpentier[35], P. Chen[3,36], N. Chiapolini[37], M. Chrzaszcz [23], K. Ciba[35], X. Cid Vidal[34], G. Ciezarek[50], P.E.L. Clarke[47], M. Clemencic[35], H.V. Cliff[44], J. Closier[35], C. Coca[26], V. Coco[38], J. Cogan[6], E. Cogneras[5], P. Collins[35], A. Comerma-Montells[33], A. Contu[15], A. Cook[43], M. Coombes[43], G. Corti[35], B. Couturier[35], G.A. Cowan[36], D. Craik[45], S. Cunliffe[50], R. Currie[47], C. D'Ambrosio[35], P. David[8], P.N.Y. David[38], I. De Bonis[4], K. De Bruyn[38], S. De Capua[51], M. De Cian[37], J.M. De Miranda[1], L. De Paula[2], W. De Silva[57], P. De Simone[18], D. Decamp[4], M. Deckenhoff[9], H. Degaudenzi[36,35], L. Del Buono[8], C. Deplano[15], D. Derkach[14], O. Deschamps[5], F. Dettori[39], A. Di Canto[11], J. Dickens[44], H. Dijkstra[35], P. Diniz Batista[1], M. Dogaru[26], F. Domingo Bonal[33,n], S. Donleavy[49], F. Dordei[11], A. Dosil Suárez[34], D. Dossett[45], A. Dovbnya[40], F. Dupertuis[36], R. Dzhelyadin[32], A. Dziurda[23], A. Dzyuba[27], S. Easo[46,35], U. Egede[50], V. Egorychev[28], S. Eidelman[31], D. van Eijk[38], S. Eisenhardt[47], U. Eitschberger[9], R. Ekelhof[9], L. Eklund[48], I. El Rifai[5], Ch. Elsasser[37], D. Elsby[42], A. Falabella[14,e], C. Färber[11], G. Fardell[47], C. Farinelli[38], S. Farry[12], V. Fave[36], D. Ferguson[47], V. Fernandez Albor[34], F. Ferreira Rodrigues[1], M. Ferro-Luzzi[35], S. Filippov[30], C. Fitzpatrick[35], M. Fontana[10], F. Fontanelli[19,i], R. Forty[35], O. Francisco[2], M. Frank[35], C. Frei[35], M. Frosini[17,f], S. Furcas[20], E. Furfaro[21], A. Gallas Torreira[34], D. Galli[14,c], M. Gandelman[2], P. Gandini[52], Y. Gao[3], J. Garofoli[53], P. Garosi[51], J. Garra Tico[44], L. Garrido[33], C. Gaspar[35], R. Gauld[52], E. Gersabeck[11], M. Gersabeck[51], T. Gershon[45,35], Ph. Ghez[4], V. Gibson[44], V.V. Gligorov[35], C. Göbel[54], D. Golubkov[28], A. Golutvin[50,28,35], A. Gomes[2], H. Gordon[52], M. Grabalosa Gándara[5], R. Graciani Diaz[33], L.A. Granado Cardoso[35], E. Graugés[33], G. Graziani[17], A. Grecu[26], E. Greening[52], S. Gregson[44], O. Grünberg[55], B. Gui[53], E. Gushchin[30], Yu. Guz[32], T. Gys[35], C. Hadjivasiliou[53], G. Haefeli[36], C. Haen[35], S.C. Haines[44], S. Hall[50], T. Hampson[43], S. Hansmann-Menzemer[11], N. Harnew[52], S.T. Harnew[43], J. Harrison[51], P.F. Harrison[45], T. Hartmann[55], J. He[7], V. Heijne[38], K. Hennessy[49], P. Henrard[5], J.A. Hernando Morata[34], E. van Herwijnen[35], E. Hicks[49], D. Hill[52], M. Hoballah[5], C. Hombach[51], P. Hopchev[4], W. Hulsbergen[38], P. Hunt[52], T. Huse[49], N. Hussain[52], D. Hutchcroft[49], D. Hynds[48], V. Iakovenko[41], P. Ilten[12], J. Imong[43], R. Jacobsson[35], A. Jaeger[11], E. Jans[38], F. Jansen[38], P. Jaton[36], F. Jing[3], M. John[52], D. Johnson[52], C.R. Jones[44], B. Jost[35], M. Kaballo[9], S. Kandybei[40], M. Karacson[35], T.M. Karbach[35], I.R. Kenyon[42], U. Kerzel[35], T. Ketel[39], A. Keune[36], B. Khanji[20], O. Kochebina[7], I. Komarov[36,29], R.F. Koopman[39], P. Koppenburg[38],

JHEP02(2013)041

M. Korolev[29], A. Kozlinskiy[38], L. Kravchuk[30], K. Kreplin[11], M. Kreps[45], G. Krocker[11], P. Krokovny[31], F. Kruse[9], M. Kucharczyk[20,23,j], V. Kudryavtsev[31], T. Kvaratskheliya[28,35], V.N. La Thi[36], D. Lacarrere[35], G. Lafferty[51], A. Lai[15], D. Lambert[47], R.W. Lambert[39], E. Lanciotti[35], G. Lanfranchi[18,35], C. Langenbruch[35], T. Latham[45], C. Lazzeroni[42], R. Le Gac[6], J. van Leerdam[38], J.-P. Lees[4], R. Lefèvre[5], A. Leflat[29,35], J. Lefrançois[7], O. Leroy[6], Y. Li[3], L. Li Gioi[5], M. Liles[49], R. Lindner[35], C. Linn[11], B. Liu[3], G. Liu[35], J. von Loeben[20], J.H. Lopes[2], E. Lopez Asamar[33], N. Lopez-March[36], H. Lu[3], J. Luisier[36], H. Luo[47], A. Mac Raighne[48], F. Machefert[7], I.V. Machikhiliyan[4,28], F. Maciuc[26], O. Maev[27,35], S. Malde[52], G. Manca[15,d], G. Mancinelli[6], N. Mangiafave[44], U. Marconi[14], R. Märki[36], J. Marks[11], G. Martellotti[22], A. Martens[8], L. Martin[52], A. Martín Sánchez[7], M. Martinelli[38], D. Martinez Santos[39], D. Martins Tostes[2], A. Massafferri[1], R. Matev[35], Z. Mathe[35], C. Matteuzzi[20], M. Matveev[27], E. Maurice[6], A. Mazurov[16,30,35,e], J. McCarthy[42], R. McNulty[12], B. Meadows[57,52], F. Meier[9], M. Meissner[11], M. Merk[38], D.A. Milanes[13], M.-N. Minard[4], J. Molina Rodriguez[54], S. Monteil[5], D. Moran[51], P. Morawski[23], R. Mountain[53], I. Mous[38], F. Muheim[47], K. Müller[37], R. Muresan[26], B. Muryn[24], B. Muster[36], P. Naik[43], T. Nakada[36], R. Nandakumar[46], I. Nasteva[1], M. Needham[47], N. Neufeld[35], A.D. Nguyen[36], T.D. Nguyen[36], C. Nguyen-Mau[36,o], M. Nicol[7], V. Niess[5], R. Niet[9], N. Nikitin[29], T. Nikodem[11], S. Nisar[56], A. Nomerotski[52], A. Novoselov[32], A. Oblakowska-Mucha[24], V. Obraztsov[32], S. Oggero[38], S. Ogilvy[48], O. Okhrimenko[41], R. Oldeman[15,d,35], M. Orlandea[26], J.M. Otalora Goicochea[2], P. Owen[50], B.K. Pal[53], A. Palano[13,b], M. Palutan[18], J. Panman[35], A. Papanestis[46], M. Pappagallo[48], C. Parkes[51], C.J. Parkinson[50], G. Passaleva[17], G.D. Patel[49], M. Patel[50], G.N. Patrick[46], C. Patrignani[19,i], C. Pavel-Nicorescu[26], A. Pazos Alvarez[34], A. Pellegrino[38], G. Penso[22,l], M. Pepe Altarelli[35], S. Perazzini[14,c], D.L. Perego[20,j], E. Perez Trigo[34], A. Pérez-Calero Yzquierdo[33], P. Perret[5], M. Perrin-Terrin[6], G. Pessina[20], K. Petridis[50], A. Petrolini[19,i], A. Phan[53], E. Picatoste Olloqui[33], B. Pietrzyk[4], T. Pilař[45], D. Pinci[22], S. Playfer[47], M. Plo Casasus[34], F. Polci[8], G. Polok[23], A. Poluektov[45,31], E. Polycarpo[2], D. Popov[10], B. Popovici[26], C. Potterat[33], A. Powell[52], J. Prisciandaro[36], V. Pugatch[41], A. Puig Navarro[36], W. Qian[4], J.H. Rademacker[43], B. Rakotomiaramanana[36], M.S. Rangel[2], I. Raniuk[40], N. Rauschmayr[35], G. Raven[39], S. Redford[52], M.M. Reid[45], A.C. dos Reis[1], S. Ricciardi[46], A. Richards[50], K. Rinnert[49], V. Rives Molina[33], D.A. Roa Romero[5], P. Robbe[7], E. Rodrigues[51], P. Rodriguez Perez[34], G.J. Rogers[44], S. Roiser[35], V. Romanovsky[32], A. Romero Vidal[34], J. Rouvinet[36], T. Ruf[35], H. Ruiz[33], G. Sabatino[22,k], J.J. Saborido Silva[34], N. Sagidova[27], P. Sail[48], B. Saitta[15,d], C. Salzmann[37], B. Sanmartin Sedes[34], M. Sannino[19,i], R. Santacesaria[22], C. Santamarina Rios[34], E. Santovetti[21,k], M. Sapunov[6], A. Sarti[18,l], C. Satriano[22,m], A. Satta[21], M. Savrie[16,e], D. Savrina[28,29], P. Schaack[50], M. Schiller[39], H. Schindler[35], S. Schleich[9], M. Schlupp[9], M. Schmelling[10], B. Schmidt[35], O. Schneider[36], A. Schopper[35], M.-H. Schune[7], R. Schwemmer[35], B. Sciascia[18], A. Sciubba[18,l], M. Seco[34], A. Semennikov[28], K. Senderowska[24], I. Sepp[50], N. Serra[37], J. Serrano[6], P. Seyfert[11], M. Shapkin[32], I. Shapoval[40,35], P. Shatalov[28], Y. Shcheglov[27], T. Shears[49,35], L. Shekhtman[31], O. Shevchenko[40], V. Shevchenko[28], A. Shires[50], R. Silva Coutinho[45], T. Skwarnicki[53], N.A. Smith[49], E. Smith[52,46], M. Smith[51], K. Sobczak[5], M.D. Sokoloff[57], F.J.P. Soler[48], F. Soomro[18,35], D. Souza[43], B. Souza De Paula[2], B. Spaan[9], A. Sparkes[47], P. Spradlin[48], F. Stagni[35], S. Stahl[11], O. Steinkamp[37], S. Stoica[26], S. Stone[53], B. Storaci[37], M. Straticiuc[26], U. Straumann[37], V.K. Subbiah[35], S. Swientek[9], V. Syropoulos[39], M. Szczekowski[25], P. Szczypka[36,35], T. Szumlak[24], S. T'Jampens[4], M. Teklishyn[7], E. Teodorescu[26], F. Teubert[35], C. Thomas[52], E. Thomas[35], J. van Tilburg[11], V. Tisserand[4], M. Tobin[37], S. Tolk[39], D. Tonelli[35], S. Topp-Joergensen[52], N. Torr[52], E. Tournefier[4,50], S. Tourneur[36], M.T. Tran[36], M. Tresch[37], A. Tsaregorodtsev[6], P. Tsopelas[38], N. Tuning[38], M. Ubeda Garcia[35], A. Ukleja[25], D. Urner[51], U. Uwer[11], V. Vagnoni[14], G. Valenti[14],

JHEP02(2013)041

R. Vazquez Gomez[33], P. Vazquez Regueiro[34], S. Vecchi[16], J.J. Velthuis[43], M. Veltri[17,g], G. Veneziano[36], M. Vesterinen[35], B. Viaud[7], D. Vieira[2], X. Vilasis-Cardona[33,n], A. Vollhardt[37], D. Volyanskyy[10], D. Voong[43], A. Vorobyev[27], V. Vorobyev[31], C. Voß[55], H. Voss[10], R. Waldi[55], R. Wallace[12], S. Wandernoth[11], J. Wang[53], D.R. Ward[44], N.K. Watson[42], A.D. Webber[51], D. Websdale[50], M. Whitehead[45], J. Wicht[35], D. Wiedner[11], L. Wiggers[38], G. Wilkinson[52], M.P. Williams[45,46], M. Williams[50,p], F.F. Wilson[46], J. Wishahi[9], M. Witek[23], W. Witzeling[35], S.A. Wotton[44], S. Wright[44], S. Wu[3], K. Wyllie[35], Y. Xie[47,35], F. Xing[52], Z. Xing[53], Z. Yang[3], R. Young[47], X. Yuan[3], O. Yushchenko[32], M. Zangoli[14], M. Zavertyaev[10,a], F. Zhang[3], L. Zhang[53], W.C. Zhang[12], Y. Zhang[3], A. Zhelezov[11], A. Zhokhov[28], L. Zhong[3], A. Zvyagin[35]

[1] *Centro Brasileiro de Pesquisas Físicas (CBPF), Rio de Janeiro, Brazil*
[2] *Universidade Federal do Rio de Janeiro (UFRJ), Rio de Janeiro, Brazil*
[3] *Center for High Energy Physics, Tsinghua University, Beijing, China*
[4] *LAPP, Université de Savoie, CNRS/IN2P3, Annecy-Le-Vieux, France*
[5] *Clermont Université, Université Blaise Pascal, CNRS/IN2P3, LPC, Clermont-Ferrand, France*
[6] *CPPM, Aix-Marseille Université, CNRS/IN2P3, Marseille, France*
[7] *LAL, Université Paris-Sud, CNRS/IN2P3, Orsay, France*
[8] *LPNHE, Université Pierre et Marie Curie, Université Paris Diderot, CNRS/IN2P3, Paris, France*
[9] *Fakultät Physik, Technische Universität Dortmund, Dortmund, Germany*
[10] *Max-Planck-Institut für Kernphysik (MPIK), Heidelberg, Germany*
[11] *Physikalisches Institut, Ruprecht-Karls-Universität Heidelberg, Heidelberg, Germany*
[12] *School of Physics, University College Dublin, Dublin, Ireland*
[13] *Sezione INFN di Bari, Bari, Italy*
[14] *Sezione INFN di Bologna, Bologna, Italy*
[15] *Sezione INFN di Cagliari, Cagliari, Italy*
[16] *Sezione INFN di Ferrara, Ferrara, Italy*
[17] *Sezione INFN di Firenze, Firenze, Italy*
[18] *Laboratori Nazionali dell'INFN di Frascati, Frascati, Italy*
[19] *Sezione INFN di Genova, Genova, Italy*
[20] *Sezione INFN di Milano Bicocca, Milano, Italy*
[21] *Sezione INFN di Roma Tor Vergata, Roma, Italy*
[22] *Sezione INFN di Roma La Sapienza, Roma, Italy*
[23] *Henryk Niewodniczanski Institute of Nuclear Physics Polish Academy of Sciences, Kraków, Poland*
[24] *AGH University of Science and Technology, Kraków, Poland*
[25] *National Center for Nuclear Research (NCBJ), Warsaw, Poland*
[26] *Horia Hulubei National Institute of Physics and Nuclear Engineering, Bucharest-Magurele, Romania*
[27] *Petersburg Nuclear Physics Institute (PNPI), Gatchina, Russia*
[28] *Institute of Theoretical and Experimental Physics (ITEP), Moscow, Russia*
[29] *Institute of Nuclear Physics, Moscow State University (SINP MSU), Moscow, Russia*
[30] *Institute for Nuclear Research of the Russian Academy of Sciences (INR RAN), Moscow, Russia*
[31] *Budker Institute of Nuclear Physics (SB RAS) and Novosibirsk State University, Novosibirsk, Russia*
[32] *Institute for High Energy Physics (IHEP), Protvino, Russia*
[33] *Universitat de Barcelona, Barcelona, Spain*
[34] *Universidad de Santiago de Compostela, Santiago de Compostela, Spain*
[35] *European Organization for Nuclear Research (CERN), Geneva, Switzerland*
[36] *Ecole Polytechnique Fédérale de Lausanne (EPFL), Lausanne, Switzerland*
[37] *Physik-Institut, Universität Zürich, Zürich, Switzerland*
[38] *Nikhef National Institute for Subatomic Physics, Amsterdam, The Netherlands*
[39] *Nikhef National Institute for Subatomic Physics and VU University Amsterdam, Amsterdam, The Netherlands*

JHEP02(2013)041

[40] NSC Kharkiv Institute of Physics and Technology (NSC KIPT), Kharkiv, Ukraine
[41] Institute for Nuclear Research of the National Academy of Sciences (KINR), Kyiv, Ukraine
[42] University of Birmingham, Birmingham, United Kingdom
[43] H.H. Wills Physics Laboratory, University of Bristol, Bristol, United Kingdom
[44] Cavendish Laboratory, University of Cambridge, Cambridge, United Kingdom
[45] Department of Physics, University of Warwick, Coventry, United Kingdom
[46] STFC Rutherford Appleton Laboratory, Didcot, United Kingdom
[47] School of Physics and Astronomy, University of Edinburgh, Edinburgh, United Kingdom
[48] School of Physics and Astronomy, University of Glasgow, Glasgow, United Kingdom
[49] Oliver Lodge Laboratory, University of Liverpool, Liverpool, United Kingdom
[50] Imperial College London, London, United Kingdom
[51] School of Physics and Astronomy, University of Manchester, Manchester, United Kingdom
[52] Department of Physics, University of Oxford, Oxford, United Kingdom
[53] Syracuse University, Syracuse, NY, United States
[54] Pontifícia Universidade Católica do Rio de Janeiro (PUC-Rio), Rio de Janeiro, Brazil, associated to[2]
[55] Institut für Physik, Universität Rostock, Rostock, Germany, associated to[11]
[56] Institute of Information Technology, COMSATS, Lahore, Pakistan, associated to[53]
[57] University of Cincinnati, Cincinnati, OH, United States, associated to[53]

[a] P.N. Lebedev Physical Institute, Russian Academy of Science (LPI RAS), Moscow, Russia
[b] Università di Bari, Bari, Italy
[c] Università di Bologna, Bologna, Italy
[d] Università di Cagliari, Cagliari, Italy
[e] Università di Ferrara, Ferrara, Italy
[f] Università di Firenze, Firenze, Italy
[g] Università di Urbino, Urbino, Italy
[h] Università di Modena e Reggio Emilia, Modena, Italy
[i] Università di Genova, Genova, Italy
[j] Università di Milano Bicocca, Milano, Italy
[k] Università di Roma Tor Vergata, Roma, Italy
[l] Università di Roma La Sapienza, Roma, Italy
[m] Università della Basilicata, Potenza, Italy
[n] LIFAELS, La Salle, Universitat Ramon Llull, Barcelona, Spain
[o] Hanoi University of Science, Hanoi, Viet Nam
[p] Massachusetts Institute of Technology, Cambridge, MA, United States

JHEP02(2013)041